



HAL
open science

Evidence for major mergers of galaxies at $z < 4$ in the VVDS and VUDS surveys

L. A. M. Tasca, O. Le Fèvre, C. Lopez-Sanjuan, P. -W. Wang, P. Cassata, B. Garilli, O. Ilbert, V. Le Brun, B. C. Lemaux, D. Maccagni, et al.

► To cite this version:

L. A. M. Tasca, O. Le Fèvre, C. Lopez-Sanjuan, P. -W. Wang, P. Cassata, et al.. Evidence for major mergers of galaxies at $z < 4$ in the VVDS and VUDS surveys. *Astronomy and Astrophysics - A&A*, 2014, 565, 10.1051/0004-6361/201321507 . hal-01442000

HAL Id: hal-01442000

<https://hal.science/hal-01442000>

Submitted on 26 Nov 2018

HAL is a multi-disciplinary open access archive for the deposit and dissemination of scientific research documents, whether they are published or not. The documents may come from teaching and research institutions in France or abroad, or from public or private research centers.

L'archive ouverte pluridisciplinaire **HAL**, est destinée au dépôt et à la diffusion de documents scientifiques de niveau recherche, publiés ou non, émanant des établissements d'enseignement et de recherche français ou étrangers, des laboratoires publics ou privés.



Distributed under a Creative Commons Attribution 4.0 International License

Evidence for major mergers of galaxies at $2 \lesssim z < 4$ in the VVDS and VUDS surveys^{*}

L. A. M. Tasca¹, O. Le Fèvre¹, C. López-Sanjuan², P.-W. Wang¹, P. Cassata¹, B. Garilli³, O. Ilbert¹, V. Le Brun¹, B. C. Lemaux¹, D. Maccagni³, L. Tresse¹, S. Bardelli⁴, T. Contini⁵, S. Charlot⁶, O. Cucciati⁴, A. Fontana⁷, M. Giavalisco⁸, J.-P. Kneib^{1,9}, M. Salvato¹⁰, Y. Taniguchi¹¹, D. Vergani¹², G. Zamorani⁴, and E. Zucca⁴

¹ Aix-Marseille Université, CNRS, LAM (Laboratoire d'Astrophysique de Marseille) UMR 7326, 13388 Marseille, France
e-mail: lidia.tasca@oamp.fr

² Centro de Estudios de Física del Cosmos de Aragón, Plaza San Juan 1, planta 2, 44001 Teruel, Spain

³ INAF – IASF, via Bassini 15, 20133 Milano, Italy

⁴ INAF – Osservatorio Astronomico di Bologna, via Ranzani, 1, 40127 Bologna, Italy

⁵ Institut de Recherche en Astrophysique et Planétologie – IRAP, CNRS, Université de Toulouse, UPS-OMP, 14 avenue E. Belin, 31400 Toulouse, France

⁶ Institut d'Astrophysique de Paris, UMR 7095 CNRS, Université Pierre et Marie Curie, 98bis boulevard Arago, 75014 Paris, France

⁷ INAF – Osservatorio Astronomico di Roma, via di Frascati 33, 00040, Monte Porzio Catone, Italy

⁸ Astronomy Department, University of Massachusetts, Amherst, MA 01003, USA

⁹ LASTRO, École polytechnique fédérale de Lausanne, Suisse

¹⁰ Max-Planck-Institut für extraterrestrische Physik, Giessenbachstrasse, 85748 Garching bei München, Germany

¹¹ Research Center for Space and Cosmic Evolution, Ehime University, Bunkyo-cho, 790–8577 Matsuyama, Japan

¹² INAF–IASF Bologna, via P. Gobetti 101, 40129 Bologna, Italy

Received 19 March 2013 / Accepted 25 February 2014

ABSTRACT

Context. The mass assembly of galaxies can proceed through different physical processes. Here we report on the spectroscopic identification of close physical pairs of galaxies at redshifts $2 \lesssim z < 4$ and discuss the impact of major mergers in building galaxies at these early cosmological times.

Aims. We aim to identify and characterize close physical pairs of galaxies destined to merge and use their properties to infer the contribution of merging processes to the early mass assembly of galaxies.

Methods. We searched for galaxy pairs with a transverse separation $r_p \leq 25 h^{-1}$ kpc and a velocity difference $\Delta v \leq 500$ km s⁻¹ using early data from the VIMOS Ultra Deep Survey (VUDS) that comprise a sample of 1111 galaxies with spectroscopic redshifts measurements at redshifts $1.8 \leq z \leq 4$ in the COSMOS, ECFDS, and VVDS–02h fields, combined with VVDS data. We analysed their spectra and associated visible and near-infrared photometry to assess the main properties of merging galaxies that have an average stellar mass $M_\star = 2.3 \times 10^{10} M_\odot$ at these redshifts.

Results. Using the 12 physical pairs found in our sample we obtain a first robust measurement of the major merger fraction at these redshifts, $f_{\text{MM}} = 19.4^{+9}_{-6}\%$. These pairs are expected to merge within 1 Gyr on average each producing a more massive galaxy by the time the cosmic star formation peaks at $z \sim 1-2$. Using the pairs' merging time scales, we derive a merging rate of $R_{\text{MM}} = 0.17^{+0.08}_{-0.05}$ Gyr⁻¹. From the average mass ratio between galaxies in the pairs, the stellar mass of the resulting galaxy after merging will be $\sim 60\%$ higher than the most massive galaxy in the pair before merging. We conclude that major merging of galaxy pairs is on-going at $2 \lesssim z < 4$ and is significantly contributing to the major mass assembly phase of galaxies at this early epoch.

Key words. galaxies: formation – galaxies: high-redshift

1. Introduction

The contribution of different physical processes to galaxy mass assembly along cosmic time is still unknown, and a clear picture describing how galaxies assemble, supported by observational evidence, has yet to emerge. Looking back at the average history

of a galaxy observed today, we are still unable to identify how and when its stellar mass has been acquired and which physical processes are possible contributors.

The mass build-up of galaxies is expected to proceed from a relatively small number of processes (for a summary, see e.g. [Springel et al. 2005b](#); [Silk & Mamon 2012](#)). New stars can form from the gas reservoir of a galaxy, either acquired at birth or replenished from a more continuous accretion process along the galaxy lifespan since formation. Major and minor merging between galaxies is identified in numerous spectacular examples in the local universe (e.g. in the RNGC catalogue, [Sulentic & Tifft 1973](#); [Barnes & Hernquist 1992](#)). Merging is efficient at assembling mass, because it produces a significant increase in mass of up to a factor of two for equal mass mergers and for each merging event. Other processes are expected to modulate

^{*} Based on data obtained with the European Southern Observatory Very Large Telescope, Paranal, Chile, under Large Programmes 070.A–9007, 177.A–0837, and 185.A–0791. Based on observations obtained with MegaPrime/MegaCam, a joint project of the CFHT and CEA/DAPNIA, at the Canada-France-Hawaii Telescope (CFHT), which is operated by the National Research Council (NRC) of Canada, the Institut National des Sciences de l'Univers of the Centre National de la Recherche Scientifique (CNRS) of France, and the University of Hawaii.

the total mass gains. AGN and SNe feedback have been proposed as mechanisms capable of quenching star formation, as well as of supporting winds that drive some mass fraction into the inter-galactic medium (IGM), hence reducing the increase in stellar mass from in-situ star formation (Silk 1997; Murray et al. 2005; Cattaneo et al. 2009). The environment of galaxies is also expected to affect mass growth, with interactions between galaxies and the dense intra-cluster medium, such as harassment or stripping, thereby rapidly removing a significant part of the gas content of a galaxy (e.g. Moore et al. 1996). These processes are expected to ultimately combine along cosmic time to produce the mass distribution observed in the well-defined Hubble sequence of galaxy types in the nearby universe.

In recent years, cold gas accretion fuelling star formation has received focussed attention, following numerical simulations (Kereš et al. 2005). In this picture, cold gas flows along the filaments of the cosmic web into the main body of a galaxy to support vigorous star formation. This mechanism has been proposed as the main mode of galaxy assembly (Dekel et al. 2009) and is often cited in recent literature as the preferred scenario for galaxy assembly (e.g. Kereš et al. 2009; Dijkstra & Loeb 2009; Bouché et al. 2010; Di Matteo et al. 2012). However, as of today, only limited and indirect observational evidence exists in support of this picture (Cresci et al. 2010; Kacprzak et al. 2012), with detailed observational investigations failing to identify direct supporting evidence (Steidel et al. 2010) until the recent claim for accretion detected at $z \sim 2$ (Bouché et al. 2013), which demonstrates the difficulty directly identifying the accretion process at work.

The merging of galaxies is another key process that contributes to galaxy assembly. The hierarchical growth of dark matter haloes is a key prediction of the Λ CDM model for galaxy formation (Davis et al. 1985; Springel et al. 2005a; Hopkins et al. 2006). In this picture, the merging of dark matter (DM) haloes would not only lead to an increase in the DM halo masses, but also naturally lead to the merging of the galaxies associated with each of the haloes (Kauffmann et al. 1993). While galaxy assembly seems to produce the more massive galaxies early in a seemingly anti-hierarchical downsizing pattern (De Lucia et al. 2006), it is nonetheless expected that merging of galaxies would continue to occur as DM haloes continue to merge along cosmic time. Since the dynamical time scale for haloes to merge is of the order of 0.5–1 Gyr (Kitzbichler & White 2008; Lotz et al. 2010), it is expected that a massive halo today, as identified in DM halo merger trees from numerical N -body simulations, will have experienced several mergers since its formation. Observational evidence of merging activity at different epochs can therefore shed light on the contribution of this process in assembling mass in galaxies.

Evidence of merging is direct and well documented. Mergers have been identified since early days of photographic galaxy atlases and classified alongside the Hubble sequence of morphological types (e.g. the RC3 catalogue, de Vaucouleurs et al. 1991). The merging process of two disc galaxies has been proposed as one of the mechanisms for producing early-type bulge-dominated galaxies, supported from simulations (e.g. Mihos & Hernquist 1996; Bournaud et al. 2005). Although this picture may be too simplistic (Bournaud et al. 2011), it is however clear that mergers do occur in the low redshift universe and that major mergers may lead to large modifications of the physical properties of the galaxies involved. Mergers are identified either a posteriori from morphological signatures like wisps, tails, or irregular shapes produced by on-going or post-merger dynamics, or a priori from the identification of pairs of physically bound

galaxies destined to coalesce. Going to high redshifts and using pairs in early merging stages rather than post-merger remnants remains the most robust way to derive a merger fraction (e.g. Le Fèvre et al. 2000). This is because major merging pairs are easier to identify at these redshifts than the post-merger morphological signatures, which are of low surface brightness and may escape detection. The pair fraction can be transformed into a merger rate per volume or per galaxy (Patton et al. 2000; Kitzbichler & White 2008; Lin et al. 2008; de Ravel et al. 2009; López-Sanjuan et al. 2011, 2013), using the dynamical time scale for a pair of galaxies with a given mass ratio and projected physical separation (Kitzbichler & White 2008; Lotz et al. 2010). The integrated merging rate over the lifespan of a galaxy since formation then gives the total amount of stellar mass assembled from the merger process.

The secure identification of pairs and measurement of pair fractions at different redshifts is therefore an important observational measurement to perform. Spectroscopic redshift measurements of both members of the pair are required to eliminate the risk of background or foreground contamination along the line of sight and confirm that the pair is physically bound. At $z \sim 1$, pairs have been observed from deep galaxy spectroscopic surveys with the confirmation of the pair nature with spectroscopic redshifts (e.g. Lin et al. 2008; de Ravel et al. 2009). From the VIMOS VLT Deep Survey (VVDS), de Ravel et al. (2009) finds that the merger fraction is higher by a factor ~ 3 at $z = 1$ than in the local Universe and further shows that the merger rate and its evolution depend significantly on the stellar mass (luminosity) of the galaxy population. At redshifts beyond $z \sim 1$, only a few direct identifications of pairs and measurements of the merger fraction and merger rate exist. López-Sanjuan et al. (2013) report a high pair fraction of ~ 20 – 22% at $1 < z < 1.8$ from 3D spectroscopy measurements in MASSIV (Mass Assembly Survey with Sinfoni in VVDS, Contini et al. 2012). At higher, redshifts Conselice et al. (2003) has used the CAS (concentration, asymmetry clumpiness) methodology, which relies on image shapes and the expected signature of on-going or past mergers, to perform a measurement of the merger fraction up to $z \sim 3$. Cooke et al. (2010) provides spectroscopic identification of five pairs of galaxies in their LBG sample at $z \sim 3$, claiming that merging is triggering a significant part of the Ly α emission. The number of confirmed pairs is therefore small beyond $z \sim 2$, and larger samples have to be assembled to enable measurements of the pair fraction and merger rate, which is accurate to a few percent.

Here we present a sample of galaxy pairs identified at $z > 1.8$ in the VIMOS Ultra Deep Survey (VUDS) and VVDS. The VUDS is an on-going survey (Le Fèvre et al. 2014) with ultra-deep spectroscopy obtained with VIMOS on the VLT targeting galaxies with $z > 2$ in three well studied fields: the COSMOS, ECDFS, and VVDS-02h (XMM-LSS/CFHTLS-D1). The VVDS has been extensively discussed elsewhere (Le Fèvre et al. 2005). We are using the “Final Data Release” of this survey as described in Le Fèvre et al. (2013b). These spectroscopic redshift survey samples are searched to identify a sample of real physical pairs with redshifts $1.8 < z < 4$, based on the observed projected separation r_p and velocity difference Δv . We discuss the derived pair properties using all available spectroscopy, as well as visible and near-IR imaging and photometric data. The VUDS and VVDS spectroscopic redshift surveys are described in Sect. 2. The methodology for identifying pairs as well as confirming that they are at close physical separation rather than a random projection along the line of sight is presented in Sect. 3. We then examine the pair properties in Sect. 4. The pair fraction

and merging rate at $1.8 < z < 4$ are discussed in Sect. 5 and we conclude in Sect. 6.

Throughout this work, we adopt a cosmology with $H_0 = 100 h \text{ km s}^{-1} \text{ Mpc}^{-1}$, $h = 0.7$, $\Omega_{0,\Lambda} = 0.73$, and $\Omega_{0,m} = 0.27$. All magnitudes are given in the AB system.

2. Spectroscopic observations and parent sample

To find pairs, we have explored the VUDS, VVDS-Deep, and VVDS-UltraDeep surveys, providing a sample of galaxies with spectroscopic redshifts measured with VIMOS on the ESO-VLT (Le Fèvre et al. 2003). The VIMOS spectra were obtained with 4.5 h of integration for the VVDS-Deep survey, covering $5500 \leq \lambda \leq 9350 \text{ \AA}$, and 16 h and 14 h integrations in each of the LRBLUE and LRRED grism settings for the VVDS-UltraDeep and VUDS surveys, respectively, covering a combined wavelength range $3600 \leq \lambda \leq 9350 \text{ \AA}$.

The VVDS-deep (Le Fèvre et al. 2005, 2013b) and VVDS-UltraDeep (Le Fèvre et al. 2013b) surveys are based on *i*-band magnitude selection with $17.5 \leq i_{AB} \leq 24$ and $23 \leq i_{AB} \leq 24.75$, each covering up to $z \sim 6$ (Le Fèvre et al. 2013a). These two VVDS surveys are located in the VVDS-02h field centred at $\alpha_{2000} = 02^{\text{h}}26^{\text{m}}00^{\text{s}}$ and $\delta_{2000} = -04 \text{ deg } 30' 00''$.

The VUDS is an on-going spectroscopic survey also using VIMOS, targeting $z > 2$ galaxies in three fields: COSMOS, ECDFS, and VVDS-02h. The baseline target selection for spectroscopy is using photometric redshifts $z_{\text{phot}} > 2.4$ measured using all the photometry available in the survey fields that use the Le Phare code (Ilbert et al. 2006). The photometric redshift accuracy obtained from the multi-wavelength data and calibrated on existing spectroscopic redshifts is $\sigma_{\delta z/(1+z)} \approx 0.01$ for magnitudes $i_{AB} < 25$ in the COSMOS field (see e.g. Ilbert et al. 2013). There is a slight degradation by a factor < 2 on the photometric redshift accuracy in the other two fields because of there are fewer photometric bands observed. In addition, we supplemented the z_{phot} selection by several colour-selection criteria, adding those galaxies likely to be in this redshift range, but not selected from the primary z_{phot} selection. Allowing for errors in z_{phot} , this selection provides a sample with $2 \lesssim z \lesssim 6$, as described in Le Fèvre et al. (2014).

All VIMOS data are processed with the VIPGI package (Scodreggio et al. 2005). Following automated measurements, each galaxy is examined visually and independently by two people, each assigning a spectroscopic redshift. These measurements are compared before assigning the final redshift measurement. A reliability flag is assigned to each redshift measurement representing the probability for the redshift to be right. As consistently shown from the VVDS (Le Fèvre et al. 2005), zCOSMOS (Lilly et al. 2007), and VIPERS (Guzzo et al. 2014) surveys, the reliability of flags reflect the statistical process of redshift assignment between independent observers and does not depend on the survey type or its intrinsic quality, with flags 1, 2, 3, 4, and 9 having a probability of being right of $\sim 50, 87, 98, 100, 90\%$, respectively. (Flags 1x with $x = 1, 2, 3, 4, 9$ indicate a broad line AGN; flag 2x are objects falling serendipitously in a slit next to a main target; and both have probability distributions similar to the main flag categories.)

Redshifts of each galaxy are measured using the EZ engine based on cross-correlating observed spectra to reference templates (Garilli et al. 2010). It is noteworthy that the redshift accuracy in spectra velocity measurements using cross-correlation is better than the instrument resolution, because, simply put, the centroid of a line can be measured to better accuracy than the

size of the resolution element, and combining a number of lines as done in the cross-correlation can improve the velocity measurement further. The accuracy of redshift measurements and associated errors have been extensively described in Le Fèvre et al. (2013b) using about 1000 independent measurements from independent observations of the same galaxies, while the measurement error for each galaxy is $\sim 200 \text{ km s}^{-1}$ and the absolute velocity accuracy of the whole sample is about 40 km s^{-1} .

In addition to the VIMOS spectroscopic data, a large set of imaging data is available in the three fields covered by our pair search. The COSMOS field (Scoville et al. 2007) has a full coverage with the HST/ACS F814W filter (Koekemoer et al. 2007) and includes, among other data, ugriz photometry from Subaru (Taniguchi et al. 2007) and, more recently, *YJHK* photometry from the UltraVista survey (McCracken et al. 2012). Spectroscopic redshifts from the zCOSMOS survey are also available (Lilly et al. 2007). The ECDFS is covered by the MUSYC survey in *UBVRIz'* (Gawiser et al. 2006) and partly by the CANDELS survey with the ACS and WFC3 on HST (Koekemoer et al. 2011). The VVDS-02h field has deep CFH12K *BVRI* photometry (Le Fèvre et al. 2004), and even deeper CFHTLS ugriz photometry (e.g. Ilbert et al. 2006), as well as *JHK* photometry from the deep survey with CFHT-WIRCAM (WIRDS Bielby et al. 2012).

At redshifts $z > 2$, most of the galaxies in VVDS and VUDS are star-forming galaxies with star-formation rates from ~ 2 to $100 M_{\odot}$, and stellar masses from $\sim 5 \times 10^9$ to $10^{11} M_{\odot}$. As discussed in Le Fèvre et al. (2013b), only the reddest galaxies are missing from the *i*-band selection of the VVDS, corresponding to heavily obscured or passive early-type galaxies. Heavily obscured objects have star formation rates comparable to the UV-selected population (Lemaux et al. 2013) so that their merging properties are expected to be similar to our UV-based selection. Since passive galaxies represent less than a few percent of the global galaxy population at $z \sim 3$ as identified from the mass function (e.g. Ilbert et al. 2013), our sample is representative of the moderately star-forming galaxy population, which is largely dominant at $z \sim 3$.

3. Pair identification

Pairs have been identified using the projected transverse separation r_p and the velocity difference $\Delta v = c(v_1 - v_2)/(1 - v_1 v_2)$ where v_x , the normalized velocity of the *x*th galaxy, is given as $v_x = [(1 + z_x)^2 - 1]/[(1 + z_x)^2 + 1]$. The survey samples have first been scanned for separation $r_p \leq 25 h^{-1} \text{ kpc}$ and $\Delta v \leq 500 \text{ km s}^{-1}$. We chose these separations because it is expected that pairs would merge in about 1 Gyr (e.g. Kitzbichler & White 2008), meaning that a pair observed at $z \sim 3$ would have merged by the peak in star formation activity at $z \sim 1.5-2$ (e.g. Cucciati et al. 2012).

Given the limitation of our ground-based seeing observations, we are not able to identify pairs superimposed along the line of sight or separated spatially by less than 1 arcsec, the average image quality (FWHM) of the imaging data, corresponding to $5 h^{-1} \text{ kpc}$ at $z \sim 3$. In addition, pairs with larger r_p or Δv could also merge, albeit on a longer time scale, and with a lower probability (Kitzbichler & White 2008).

We used all objects with reliability flags 2 to 9 (galaxies) and 12 to 19 (broad-line AGN) for the primary targets, including a total of 1111 galaxies, and an additional 811 galaxies with flags 1 to 9 and 11 to 19, as well as 21 to 29 (objects falling serendipitously in the slit), for the companions.

Table 1. Pair properties.

Field	Pair galaxies ID numbers	Redshift z_1	Stellar masses ¹ $10^{10} M_{\odot}$	Mass ratio ²	Flux ratio ³	r_p ⁴ h^{-1} kpc	Δv ⁵ km s^{-1}	T_{merg} ⁶ Gyr	z_{assembly} ⁷
COSMOS	511001467 a&b	2.0970	0.3/0.15	2.0	1.9 ± 0.2	18.4 ± 0.3	87	2.3	1.1
	510788270 a&b	2.9629	0.5/0.7	1.4	1.7 ± 0.3	15.4 ± 0.2	38	1.5	1.8
	510175610/510778438	3.0939	0.8/5.0	6.3	4.2 ± 0.2	9.4 ± 0.2	161	0.7	2.3
VVDS-02h	520452183/520450423	1.8370	5.6/3.0	1.9	2.2 ± 0.1	22.3 ± 1.2	390	1.1	1.3
	520478238/520478087	2.2460	2.0/1.0	2.0	1.8 ± 0.4	25.3 ± 1.2	28	1.8	1.3
	910260902/910261083	2.3594	3.4/7.9	2.3	2.0 ± 0.1	12.3 ± 1.1	54	0.6	1.9
	910302317/910302929	1.8171	1.1/1.8	1.6	1.4 ± 0.1	8.7 ± 1.2	181	0.6	1.5
ECDFS	530034527 a&b	3.6500	1.2/0.9	1.3	1.5 ± 0.1	6.6 ± 0.2	0	0.5	2.9
	530050663 a&b	2.3250	0.4/0.2	2.0	1.9 ± 0.2	5.5 ± 0.3	54	0.6	1.9
	530042814/530042840	2.9903	0.12/0.1	1.2	1.3 ± 0.1	6.0 ± 0.2	278	1.0	2.1
	530046916 a&b	2.8684	1.4/0.6	2.3	2.5 ± 0.1	6.5 ± 0.2	279	0.5	2.4
	530036900 a&b	3.3300	1.3/1.1	1.2	1.5 ± 0.1	7.0 ± 0.2	76	0.6	2.6

Notes. ⁽¹⁾ Stellar mass estimates from SED fitting; ⁽²⁾ stellar mass ratio between the two galaxies in the pair, errors on the mass ratio have been computed from the error on the ratio of the H or K band flux measurements (see text); ⁽³⁾ flux ratio as measured on H or K -band; ⁽⁴⁾ r_p : transverse separation between the two galaxies in the pair, errors in r_p have been conservatively estimated taking a one pixel error on the difference in the centroid measurement of each galaxy in the pair; ⁽⁵⁾ Δv : velocity separation along the line of sight; errors in Δv are estimated to be $<100 \text{ km s}^{-1}$ when the two redshifts are from the same slit (10 pairs), and $\sim 200 \text{ km s}^{-1}$ when redshifts are from two different slits (2 pairs); ⁽⁶⁾ T_{merg} : time scale for the pair to merge, using the Kitzbichler & White (2008) prescription; from errors in mass ratio, r_p and Δv errors on T_{merg} are $\sim 10\text{--}20\%$; ⁽⁷⁾ z_{assembly} : redshift by which the two galaxies will have merged, obtained combining the observed redshift and the Δz corresponding to the merger time scale.

In looking for pairs, there is a possibility that the two identified objects could be two giant HII regions of the same galaxy, which would then be prominent in the UV rest frame probed by the i -band, but which would appear as a single galaxy in the H or K band, which probes red-wards of the D4000 or Balmer breaks at wavelengths that are less sensitive to contamination by younger stellar populations. In contrast, the persistence of separate morphological components in the redder bands is an indication of the existence of two galaxies even if they are embedded in a diffuse light background. We therefore examined the i -band and H/K -band images of the pair candidates selected from their separation. As described in the next section, all of our pairs are well separated, and both galaxies are seen from bluer to redder bands. We are therefore confident that we are dealing with true physical pairs rather than double HII regions of the same galaxy.

In this process, we have identified 12 pairs with redshifts from $z = 1.82$ to $z = 3.65$. All primary and companion galaxies have flags ≥ 2 except one companion galaxy (ID: 520478087) with a lower reliability flag 1. Our pair sample therefore benefits from reliable spectroscopic identification. The pair properties are discussed in the next section.

4. Pair properties

From the multi-wavelength dataset, we have derived the main properties of the galaxies in the identified pairs. An important parameter for this study is the stellar mass ratio used to separate “major-merging pairs”, with a mass ratio between the two galaxies of $1 \leq M_1/M_2 \leq 4$, from “minor-merging pairs”, for which $M_1/M_2 > 4$. To measure this ratio, we used two different approaches and verified that they provide the same sample of major-merging pairs. First, the stellar mass of each galaxy of a pair has been derived from SED fitting of the available photometric data at the measured redshift (see e.g. Ilbert et al. 2010) and range from 10^9 to $10^{11} M_{\odot}$ (Table 1). While this method is known to lead to absolute uncertainties of up to a factor 2 (e.g. Bolzonella et al. 2010) depending on the number of bands used

or on the IMF, the relative comparisons of masses derived from this method are robust when derived from the same set of SED models, since it is mainly the mass scaling that changes (e.g. Ilbert et al. 2013).

Since our major-merger sample is selected based on a mass ratio, we investigated how our sample would be affected by systematic errors on the mass ratio. To verify the robustness of our major pair sample to the SED-derived mass ratio, we computed the flux ratio of each pair using the K -band (or H -band when not available) flux of each component of a pair. The luminosity of a galaxy above $\lambda_{\text{rest}} \gtrsim 4000 \text{ \AA}$ can be considered as a rough proxy for stellar mass because it is the most sensitive to the older stellar populations accumulated over the life of a galaxy (Bruzual & Charlot 2003), and therefore the flux ratios should be close to a mass ratio. The flux ratios are reported in Table 1 and are in excellent agreement with the SED-derived mass ratio. Given the agreement between these two methods, we used the error on the K -band (or H -band) flux ratio as a proxy for mass ratio errors, which is easier to control than the SED-derived mass ratio error, with typical errors ranging from 0.1 to 0.4 for the faintest pairs. The distribution of mass ratio reported in Table 1 indicates that all pairs have a mass ratio $M_1/M_2 \leq 2.5$, which is consistent with their flux ratio and well above our $M_1/M_2 \leq 4$ limit. Therefore given the 1σ uncertainties on flux ratio estimates reported in Table 1 it is unlikely that any of the major merger pairs are misclassified minor mergers. We conclude from this analysis that our major-merger pair sample is not affected by stellar mass ratio uncertainties. Because our primary galaxy sample is to first order magnitude-selected and galaxies are star-forming with similar SEDs, the magnitude limit ranging from $i_{AB} = 24$ to 25 corresponds to a stellar-mass limit in the range $M_{*} = 10^9$ to $5 \times 10^9 M_{\odot}$ depending on redshift over the redshift range considered.

Taking the mass ratio between the two galaxies in a pair into account, along with the separations Δv and r_p , we used the formalism of Kitzbichler & White (2008, formula 10) to compute the merging time scale for each pair T_{merg} , as described in

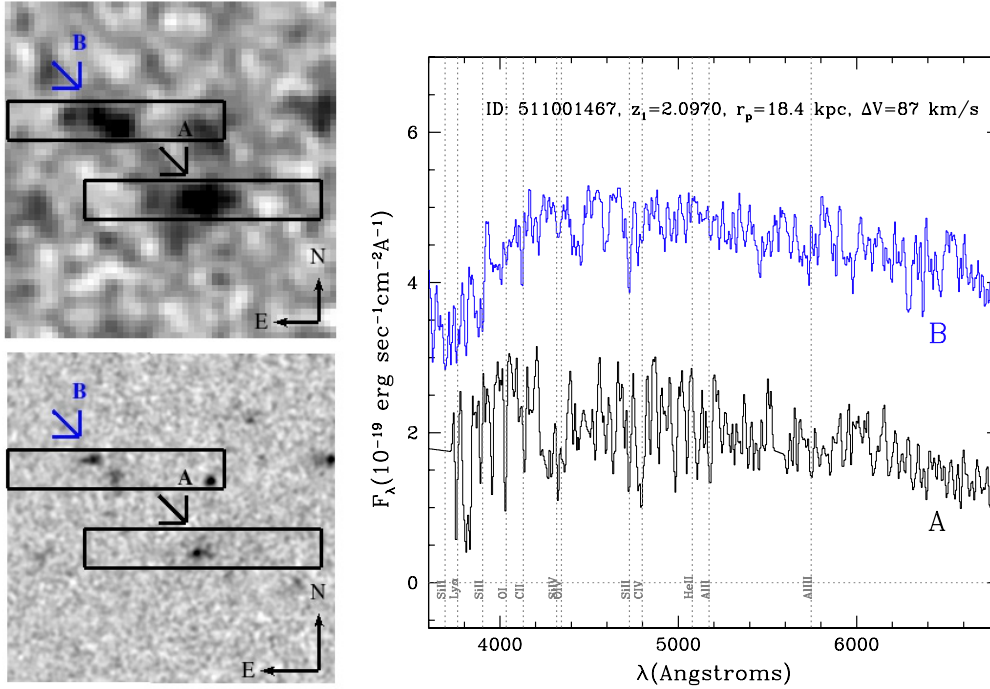


Fig. 1. Pair COSMOS-511001467 A/B: $5'' \times 5''$ sum of UltraVista YJHK images (*top-left*) and HST F814W image (*bottom left*). The location of the 1 arcsec width VLT/VIMOS slits is shown by the rectangles. The more massive object is labelled as A. *Right panel*: VIMOS spectra for both components in the pair. The spectra have been arbitrarily shifted in flux to avoid overlap.

de Ravel et al. (2009). These time scales are compatible with the Lotz et al. (2010) estimates, as discussed in López-Sanjuan et al. (2011). We list the main pair properties in Table 1, including T_{merg} and the redshift z_{assembly} by which the pair would have merged into a single galaxy, taking the redshift of the pair and T_{merg} into account. Images and spectra of each pair are presented in Figs. 1 to 12. We describe the properties of each pair below.

COSMOS-511001467 A/B (Fig. 1): redshifts of the two galaxies in this pair have been measured from two different VUDS observations at $z_1 = 2.0970$ and $z_2 = 2.0961$, for a velocity difference of $\Delta v = 87 \text{ km s}^{-1}$. The two galaxies are separated by $18.4 h^{-1} \text{ kpc}$, and are easily visible both in the HST/ACS F814W image and in the UltraVista near-infrared images. The most massive galaxy has a stellar mass of $0.3 \times 10^{10} M_{\odot}$, and the stellar mass ratio between the two galaxies is estimated to be $M_1/M_2 = 2$, hence a major merger. The south-west galaxy shows a compact nucleus surrounded by a faint diffuse component, while the north-eastern galaxy is seen as two components in both HST/ACS F814W and UltraVista images. The spectra of the two galaxies have a UV flux rising to the blue up to Ly α , typical of star-forming galaxies at these redshifts. Given the physical separation and mass difference, and following the prescription of Kitzbichler & White (2008), this pair is expected to merge within 2.3 Gyr.

COSMOS-510788270 A/B (Fig. 2): two galaxies separated by $15.4 h^{-1} \text{ kpc}$ are at a redshift $z = 2.9629$ with a velocity difference $\Delta v = 38 \text{ km s}^{-1}$, measured from two different VUDS observations. The most massive galaxy has a mass $0.7 \times 10^{10} M_{\odot}$, and the mass ratio between the two galaxies is estimated to be $M_1/M_2 = 1.5$, so a major merger. One of the spectra shows Ly α in emission with $EW(\text{Ly}\alpha)_{\text{rest}} = 15 \text{ \AA}$, while Ly α is observed in absorption for the other galaxy. Images are barely resolved at the HST/ACS resolution, showing a slightly extended and elliptical light distribution. This pair is expected to merge within 1.5 Gyr.

COSMOS-510175610/510778438 (Fig. 3): this pair at a redshift $z_1 = 3.0939$ is separated by $9.4 h^{-1} \text{ kpc}$ and $\Delta v = 161 \text{ km s}^{-1}$, measured in the same slit from VUDS observations. The brightest and most massive galaxy has a compact, although irregular, morphology, while the companion to the west, which is confirmed at the same redshift, is more diffuse and has a low surface brightness. Another companion is visible about $3 h^{-1} \text{ kpc}$ to the north-east, and although its photometry is compatible with the redshift of the pair, no spectroscopic redshift information is available to confirm that it is physically linked to this system. Both spectra have been obtained from the VUDS survey. One of the VIMOS spectra shows a weak Ly α in emission, while the other is purely in absorption. The mass of the brightest galaxy is $5 \times 10^{10} M_{\odot}$, and the mass ratio is $M_1/M_2 = 6.3$, considered to be a minor merger. This pair is expected to merge within 0.7 Gyr.

VVDS-02h-520452183/520450423 (Fig. 4): the spectra of these two galaxies obtained from the same VVDS slit show a broad-line AGN with $z = 1.8370$ and an absorption-line galaxy with $z = 1.8333$ for a velocity difference $\Delta v = 391 \text{ km s}^{-1}$. This pair is separated by $22.3 h^{-1} \text{ kpc}$, and the estimated mass ratio is $M_1/M_2 = 1.9$, with the most massive galaxy, the AGN host, having a stellar mass $5.6 \times 10^{10} M_{\odot}$. This estimate is, however, quite uncertain given the presence of the AGN. Another object is observed in between the two main galaxies, but no redshift information is available. The AGN host is compact, barely resolved at the seeing of the best CFHTLS image ($FWHM = 0.6 \text{ arcsec}$), while the companion galaxy is slightly elongated and irregular in shape. Given the physical separation and mass difference, this pair is expected to merge within 1.1 Gyr, although this estimate is affected by the uncertain mass estimate of the AGN host.

VVDS-02h-520478238/520478087 (Fig. 5): the two galaxies observed spectroscopically in the same VUDS slit have $z_1 = 2.2460$, $z_2 = 2.2463$ for a velocity difference $\Delta v = 28 \text{ km s}^{-1}$, and are separated by $r_p = 25 h^{-1} \text{ kpc}$. They are part of a group

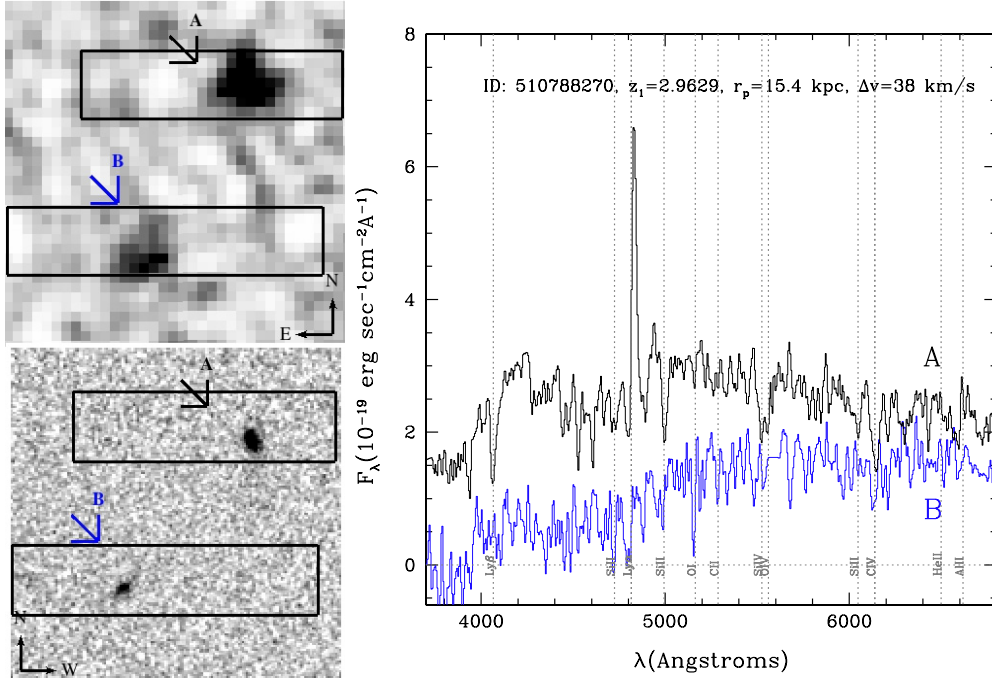


Fig. 2. Pair COSMOS-510788270 A/B: $5'' \times 5''$ sum of UltraVista YJHK images (*top-left*) and HST F814W image (*bottom left*). The location of the 1 arcsec width VLT/VIMOS slits is shown by the rectangles. The more massive object is labelled as A. *Right panel*: VIMOS spectra for both components in the pair. The spectra have been arbitrarily shifted in flux to avoid overlap.

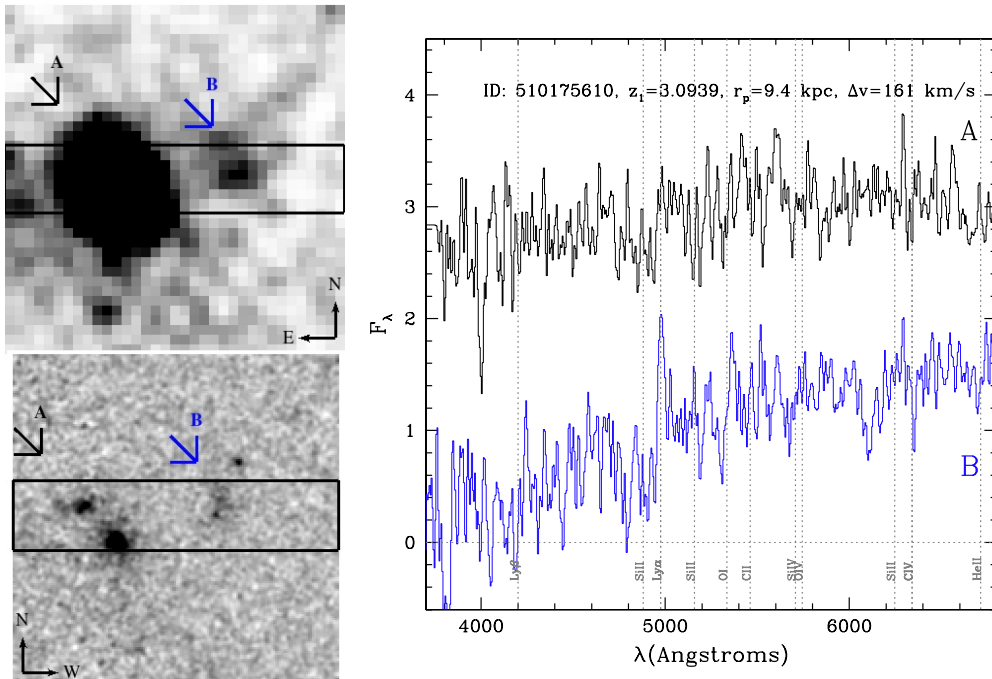


Fig. 3. Pair COSMOS-510175610/510778438: $5'' \times 5''$ sum of UltraVista YJHK images (*top-left*) and the HST F814W image (*bottom left*). The location of the 1 arcsec width VLT/VIMOS slit is shown by the rectangle. The more massive object is labelled as A. *Right panel*: VIMOS spectra for both components in the pair. The spectra have been arbitrarily shifted in flux to avoid overlap.

of four galaxies within 5 arcsec ($30 h^{-1}$ kpc), with photometric redshifts compatible with the redshift of the pair. The eastern component is the most massive with $M_{\star} = 2.0 \times 10^{10} M_{\odot}$. The mass ratio, $M_1/M_2 = 2$, indicates a major merger and results in an expected time to merge within 1.8 Gyr.

VVDS-02h-910260902/910261083 (*Fig. 6*): the two galaxies, spectroscopically observed in the same VVDS slit with $z_1 = 2.3594$ and $z_2 = 2.3588$, are identified both in the

CFHTLS *i*-band image and the *K*-band WIRDS image, with an $r_p = 12.3 h^{-1}$ kpc and $\Delta v = 54 \text{ km s}^{-1}$ separation. The slit was placed on the centroid of the blended CFHTLS image of the two galaxies, but still included a significant fraction of the flux of both galaxies to yield two well separated spectra. The south-east galaxy is the most massive with $7.9 \times 10^{10} M_{\odot}$ and the mass ratio is $M_1/M_2 = 2.4$, the later indicating a major merger. While the massive galaxy shows a symmetric elongated shape,

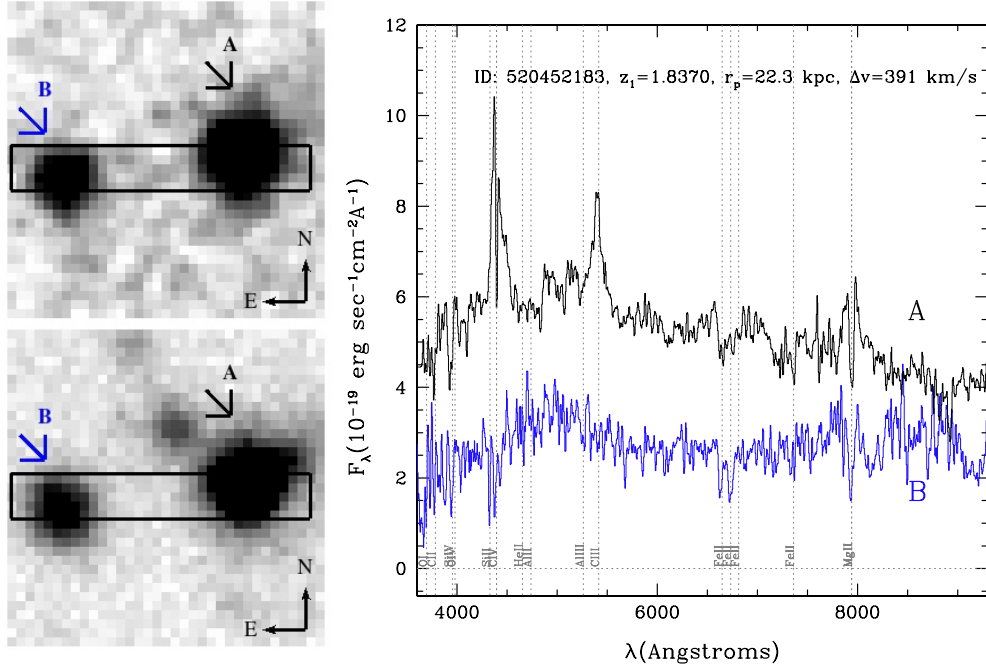


Fig. 4. Pair VVDS-2h-520452183/520450423: $6.5'' \times 6.5''$ composite WIRDS JHKs image (*top-left*) and CFHTLS *i*-band image (*bottom left*). The location of the 1 arcsec width VLT/VIMOS slit is shown by the rectangle. The more massive object is labelled as A. *Right panel*: VIMOS spectra for both components in the pair. The spectra have been arbitrarily shifted in flux to avoid overlap.

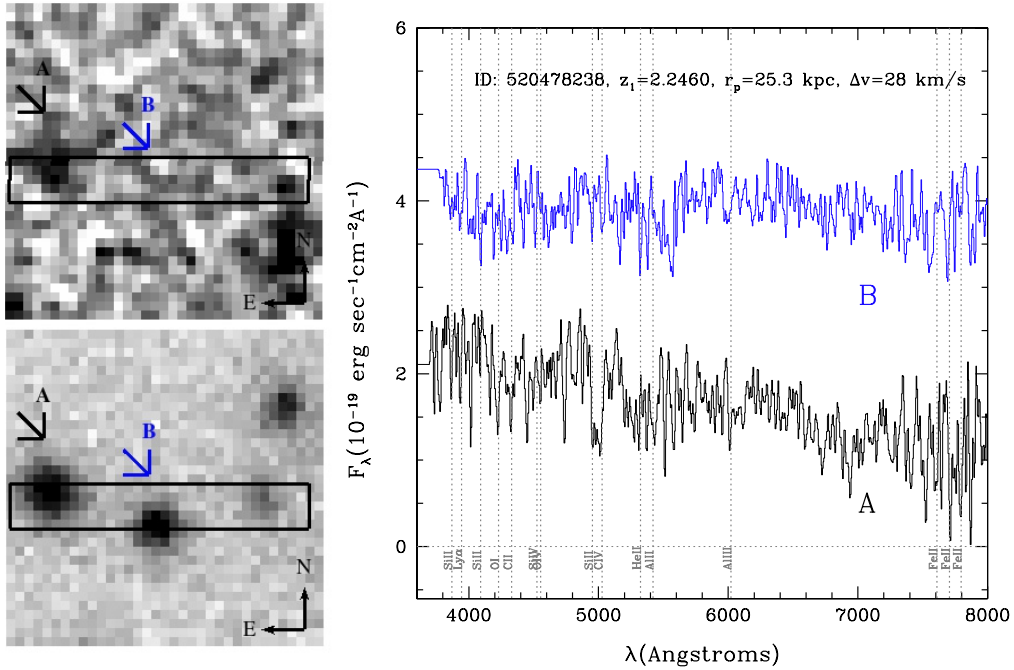


Fig. 5. Pair VVDS-2h-520478238/520478087: $6.5'' \times 6.5''$ composite WIRDS JHKs image (*top-left*) and CFHTLS *i*-band image (*bottom left*). The location of the 1 arcsec width VLT/VIMOS slit is shown by the rectangle. The more massive object is labelled as A. *Right panel*: VIMOS spectra for both components in the pair. The spectra have been arbitrarily shifted in flux to avoid overlap.

the north-west galaxy shows an irregular morphology, and the two are connected by a faint bridge. Both galaxies show $\text{Ly}\alpha$ in emission, with $EW(\text{Ly}\alpha)_{\text{rest}} = 50 \text{ \AA}$ and 60 \AA , and integrated $\text{Ly}\alpha$ line flux $L_{\text{Ly}\alpha} = 10^{42}$ and $3 \times 10^{42} \text{ erg s}^{-1}$, respectively, indicating strong star formation at the level of $1\text{--}2 M_{\odot}/\text{yr}$ (see e.g. Cassata et al. 2011). Given the observed separation of this pair, it is expected that it will merge within 0.6 Gyr.

VVDS-02h-910302317/910302929 (*Fig. 7*): the two main galaxies observed in spectroscopy in the same VVDS slit are at $z_1 = 1.8171$ and $z_2 = 1.8154$, respectively, separated by $8.7 h^{-1} \text{ kpc}$ along the east-west direction, and by $\Delta v = 181 \text{ km s}^{-1}$. The brightest/most massive galaxy has a mass $1.8 \times 10^{10} M_{\odot}$ and is made of two main components, visible in both the *i*-band and *K*-band images. The mass ratio between

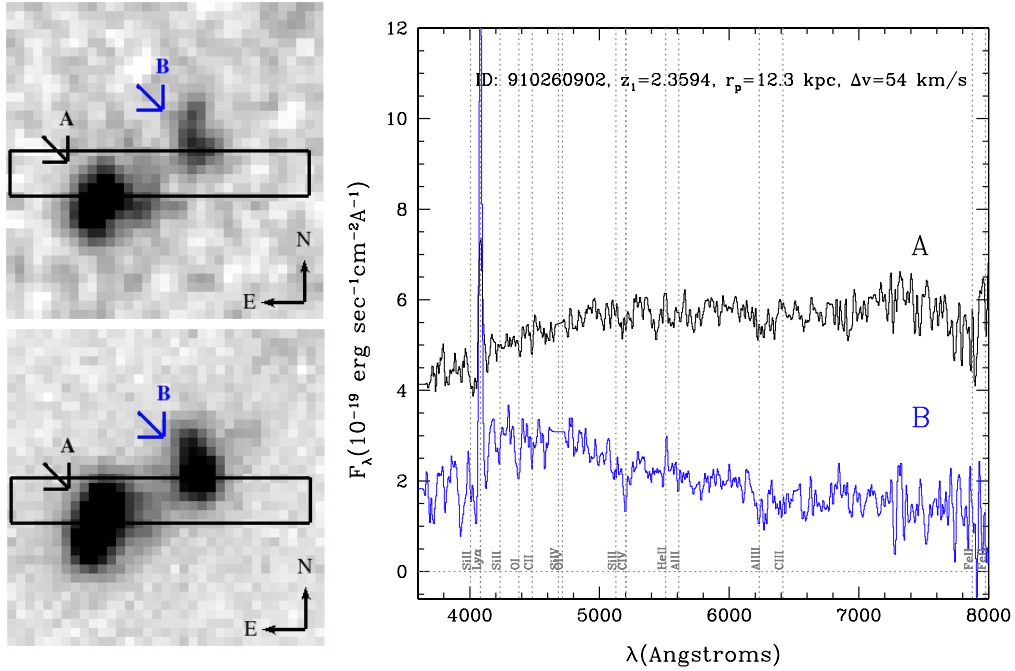


Fig. 6. Pair VVDS-2h-910260902/910261083: $6.5'' \times 6.5''$ composite WIRDS *JHKs* image (*top-left*) and CFHTLS *i*-band image (*bottom-left*). The location of the 1 arcsec width VLT/VIMOS slit is shown by the rectangle. The more massive object is labelled as A. *Right panel*: VIMOS spectra for both components in the pair. The spectra have been arbitrarily shifted in flux to avoid overlap.

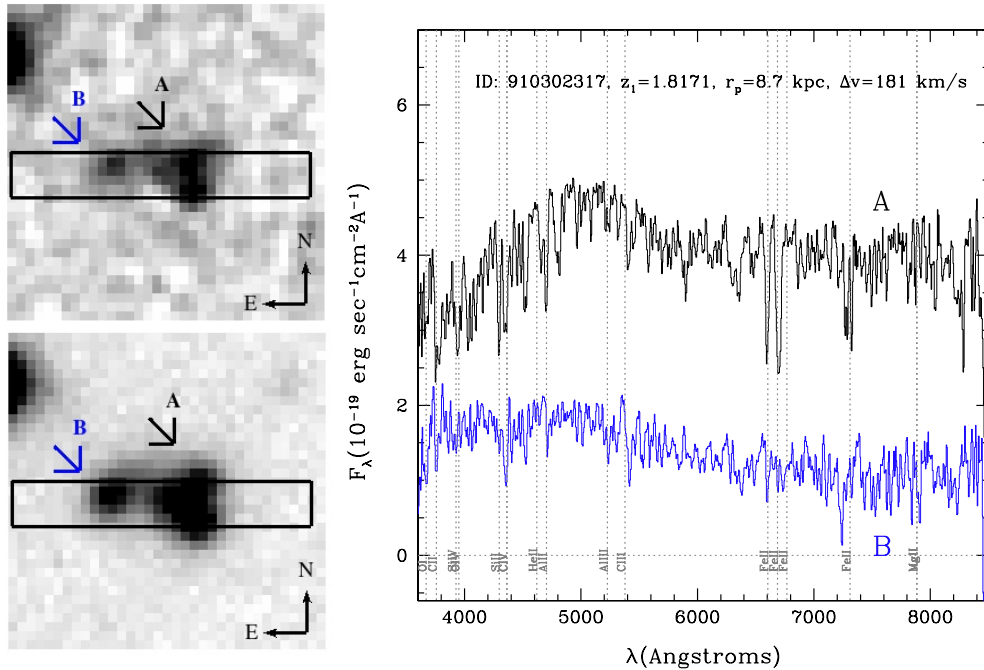


Fig. 7. Pair VVDS-2h-910302317/910302929: $6.5'' \times 6.5''$ composite WIRDS *JHKs* image (*top-left*) and CFHTLS *i*-band image (*bottom left*). The location of the 1 arcsec width VLT/VIMOS slit is shown by the rectangle. The more massive object is labelled as A. *Right panel*: VIMOS spectra for both components in the pair. The spectra have been arbitrarily shifted in flux to avoid overlap.

the two galaxies in the pair is $M_1/M_2 = 1.7$, which indicates a major merger. This pair is expected to merge within 0.6 Gyr.

ECDFS-530034527 (Fig. 8): this is the highest redshift for which we have obtained a spectroscopic confirmation of a physical pair, with both galaxies at the same redshift $z = 3.6500$, separated by $6.8 h^{-1}$ kpc, as measured from the same VUDS slit. In Fig. 8 another companion is observed to the north-east, but there is no confirmation of its redshift. The stellar mass of the

brightest and most massive galaxy is $1.2 \times 10^{10} M_\odot$, and the mass ratio with the companion is $M_1/M_2 = 1.3$, which indicates a major merger. The two spectra obtained in the VUDS survey show absorption line spectra, with only a weak Ly α emission for the brighter galaxy. This pair is expected to merge within 0.5 Gyr.

ECDFS-530050663 (Fig. 9): this pair is made of two components identified in the *H*-band CANDELS image, with redshifts

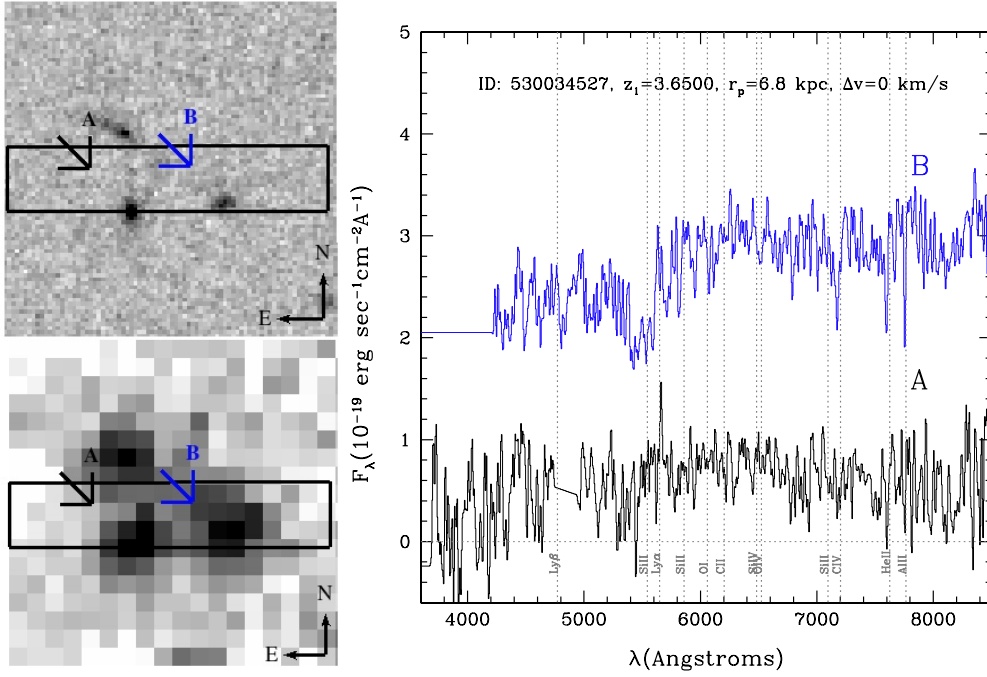


Fig. 8. Pair ECDFS-530034527 A/B: $5'' \times 5''$ HST/WFC3 F160W CANDELS image (*top-left*) and composite BVR image from the MUSYC survey MUSYC (*bottom left*). The location of the 1 arcsec width VLT/VIMOS slit is shown by the rectangle. The more massive object is labelled as A. *Right panel*: VIMOS spectra for both components in the pair. The spectra have been arbitrarily shifted in flux to avoid overlap.

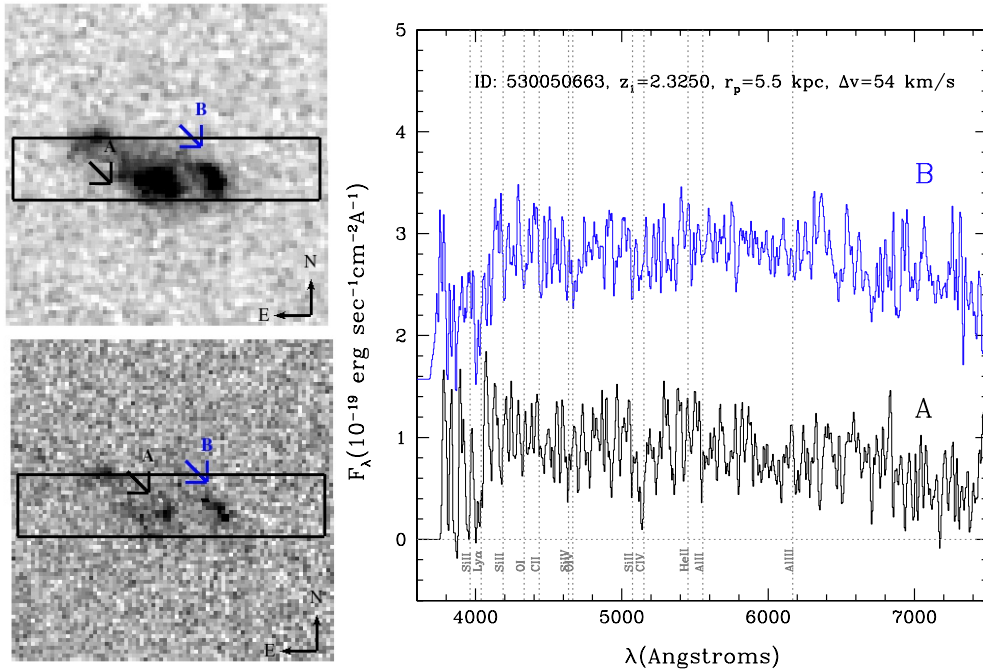


Fig. 9. Pair ECDFS-530050663 A/B: $5'' \times 5''$ HST/WFC3 F160W image (*top-left*) and HST/ACS F850W image from the CANDELS survey (*bottom left*). The location of the 1 arcsec width VLT/VIMOS slit is shown by the rectangle. The more massive object is labelled as A. *Right panel*: VIMOS spectra for both components in the pair. The spectra have been arbitrarily shifted in flux to avoid overlap.

$z_1 = 2.3250$ and $z_2 = 2.3244$ measured in the same VUDS slit. The stellar mass of the main component is $0.4 \times 10^{10} M_{\odot}$, and the mass ratio between components is $M_1/M_2 = 2$: a major merger. A third component is observed to the north-east, all three components being embedded in a low surface brightness emission. The pair identification is therefore ambiguous, since this configuration might be indeed a merger at an advanced stage surrounded by tidal debris, or the result of three giant star-forming regions

in a single forming galaxy. Under the merger hypothesis, the two main components are expected to merge within 0.6 Gyr.

ECDFS-530042814/530042840 (*Fig. 10*): the two galaxies are seen very well in the composite BVR MUSYC images and the K -band image. These galaxies are at a mean redshift $z = 2.9903$ with a velocity difference $\Delta v = 278 \text{ km s}^{-1}$ as measured in the same VUDS slit. These two main galaxies are separated by $6 h^{-1} \text{ kpc}$, and a third component is observed $6.5 h^{-1} \text{ kpc}$

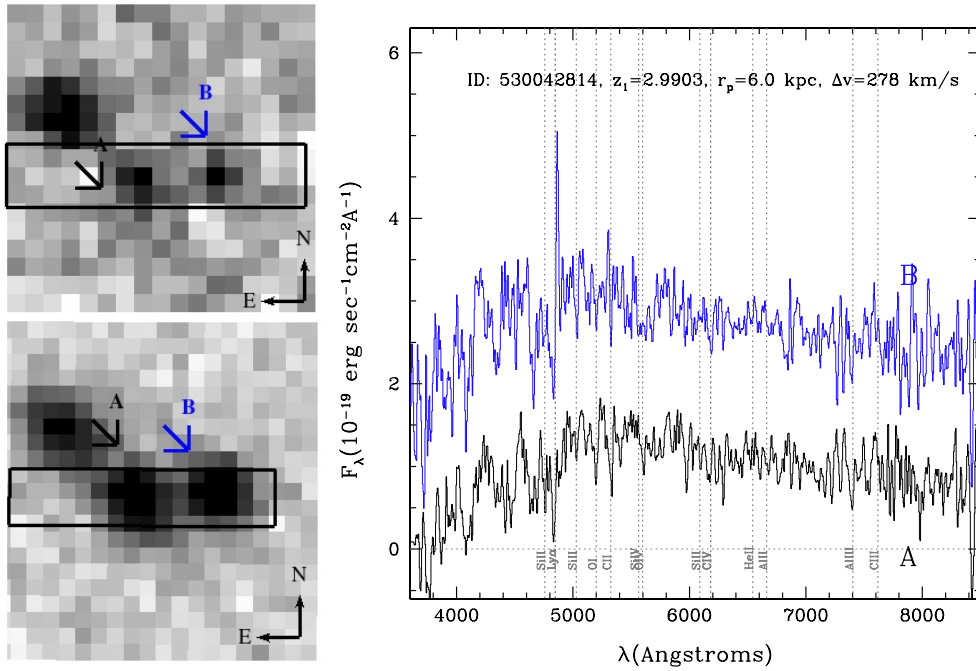


Fig. 10. Pair ECDFS-530042814/530042840: $5'' \times 5''$ composite *JK* image (*top-left*) and composite *BVR* image from the MUSYC survey (*bottom left*). The location of the 1 arcsec width VLT/VIMOS slit is shown by the rectangle. The more massive object is labelled as A. *Right panel*: VIMOS spectra for both components in the pair. The spectra have been arbitrarily shifted in flux to avoid overlap.

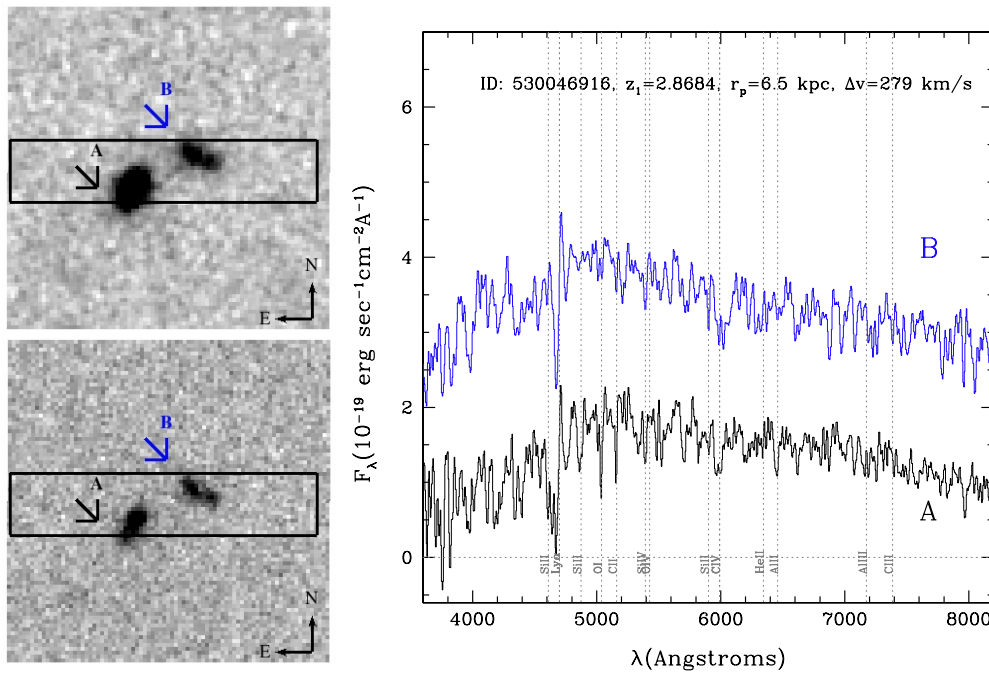


Fig. 11. Pair ECDFS-530046916 A/B: $5'' \times 5''$ HST/WFC3 F160W image (*top-left*) and HST/ACS F850W image from the CANDELS survey (*bottom left*). The location of the 1 arcsec width VLT/VIMOS slit is shown by the rectangle. The more massive object is labelled as A. *Right panel*: VIMOS spectra for both components in the pair. The spectra have been arbitrarily shifted in flux to avoid overlap.

the north-east. While the main galaxy shows Ly α in absorption, the other galaxy measured with VIMOS shows Ly α in emission, both spectra having a UV slope indicating strong star formation. The mass of the main galaxy is estimated to be $0.12 \times 10^{10} M_{\odot}$, and the mass ratio is $M_1/M_2 = 1.2$ almost an equal mass major merger. This pair is expected to merge within 1.0 Gyr.

ECDFS-530046916 (Fig. 11): two close but well separated images of two galaxies are observed in both HST z -band (F850W) and H -band (F160W) images, with a redshift around $z = 2.868$ measured in the same VUDS slit. The brightest/most massive galaxy has a regular morphology compatible with a disc, while the companion galaxy has an irregular shape. The mass of the main galaxy is estimated to be $1.4 \times 10^{10} M_{\odot}$, and the mass

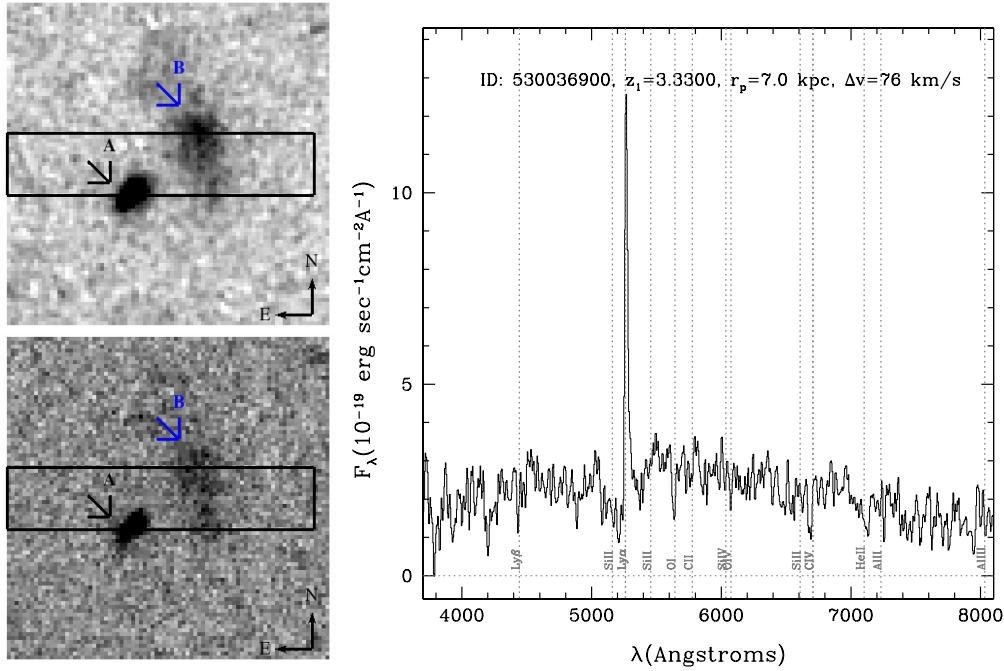


Fig. 12. Pair ECDFS-530036900 A/B: $5'' \times 5''$ HST/WFC3 F160W image (*top-left*) and HST/ACS F850W image from the CANDELS survey (*bottom left*). The location of the 1 arcsec width VLT/VIMOS slit is shown by the rectangle. The more massive object is labelled as A. *Right panel*: VIMOS VUDS spectrum for component A. The redshift of component B has been measured by Popesso et al. (2009) and not shown in the figure.

ratio is $M_1/M_2 = 2.3$, indicating a major merger. This pair will probably merge within 0.5 Gyr.

ECDFS-530036900/26931 (*Fig. 12*): two well separated galaxies are observed in the HST z -band (F850W) and H -band (F160W) images from CANDELS, with $7.0 h^{-1}$ kpc and $\Delta v = 78 \text{ km s}^{-1}$ separation at a redshift of $z_1 = 3.3300$. One galaxy is quite compact, while the companion shows a sharp point-like component surrounded by a nebulous extension. The compact galaxy has been observed by VUDS and shows strong Ly α emission, while the fainter galaxy has been observed as part of the VIMOS-GOODS survey (Popesso et al. 2009). The mass of the main galaxy is estimated to be $1.3 \times 10^{10} M_{\odot}$, and the mass ratio is $M_1/M_2 = 1.2$, an almost equal mass major merger. This pair will probably merge in less than 0.6 Gyr.

5. The pair fraction and merging rate at $2 \lesssim z < 4$

From the identified pairs, we derive a first robust measurement of the major merger pair fraction at these redshifts. This requires a complete understanding of the survey selection function, including the target selection, spatial sampling, and spectroscopic success rate. We follow the same method as described in de Ravel et al. (2009, 2011) and López-Sanjuan et al. (2011), as the instrumental set-up using VIMOS is identical. The pairs have been identified from a parent photometric sample used for selecting targets in the VUDS and VVDS. The probability of selecting a galaxy from this parent sample is the target sampling rate (TSR), defined as the ratio $\text{TSR} = N_{\text{target}}/N_{\text{phot}}$ of N_{target} objects targeted in the spectroscopic observations over N_{phot} the number of objects in the parent photometric catalogue. The TSR of the VVDS sample has been described in Le Fèvre et al. (2013b) and varies from 6.5% for the Ultra-Deep sample and up to 29% for the Deep sample. For the VUDS sample, we have computed the TSR using the parent photometric catalogue used in selecting targets for the first set of existing observations. In the redshift

range probed here, we find a $\text{TSR}_{\text{VUDS}} = 10\%$, independent of magnitude. Once targeted for VIMOS observations, an object has an associated probability of having a measured spectroscopic redshift, defined as the spectroscopic success rate (SSR). The SSR is computed as the ratio $\text{SSR} = N_{\text{spec}}/N_{\text{target}}$ where N_{spec} is the number of objects with a spectroscopic redshift measurement. In both VVDS and VUDS, we have been using a flag system related to the probability of the redshift being correct, as described extensively in Le Fèvre et al. (2013b). As the VUDS observational set-up is nearly identical to that of the VVDS, we used the SSR of the VVDS-Ultra Deep sample with an average $\text{SSR} = 80\%$ (Le Fèvre et al. 2013b). In addition, we need to apply a correction factor accounting for the ground-based seeing-limited observations that prevent us from observing pairs separated by less than one arcsecond on the plane of the sky, the average image quality of the spectroscopic observations. This is computed as the ratio of the number of spectroscopic pairs over the number of photometric pairs in the parent photometric catalogue.

Following de Ravel et al. (2009) and López-Sanjuan et al. (2011), we obtain the pair fraction as $f_{\text{MM}} = N_{\text{p}}/N_1$, where $N_1 = 1111$ is the number of principal galaxies, and N_{p} is the corrected number of pairs

$$N_{\text{p}}/N_1 = \frac{\sum_{k=1}^{N_{\text{p,obs}}} w_{\text{spec},1}^k \times w_{\text{spec},2}^k \times w_{\text{comp}}^k \times w_{\theta}^k}{\sum_{i=1}^{N_{\text{p,obs}}} w_{\text{spec}}^i}$$

assuming w_{spec} approximately constant, this leads to

$$N_{\text{p}}/N_1 = \frac{w_{\text{spec}}^2 \sum_k w_{\theta}^k \times w_{\text{comp}}^k}{w_{\text{spec}} \sum_i 1} = \frac{w_{\text{spec}} \sum_k w_{\theta}^k \times w_{\text{comp}}^k}{1111}$$

where w_{spec} is computed for each field as $w_{\text{spec}} = 1/\text{TSR} \times 1/\text{SSR}$, with $w_{\text{spec}}(\text{COSMOS}) = 0.124$, $w_{\text{spec}}(\text{VVDS}) = 0.089$ and $w_{\text{spec}}(\text{ECDFS}) = 0.081$.

Here, w_{comp} is estimated for each pair as $\rho(M_2)/\rho(M_{\text{lim}})$ where $\rho(M_2)$ is the number density of galaxies with stellar mass higher than $M_2 = M_1 \times (1/4)$, M_1 is the stellar mass of the more massive galaxy in the pair, 1/4 is the major merger ratio, $\rho(M_{\text{lim}})$ is the number density of galaxies with stellar mass higher than the mass limit of the survey at each redshift, and number densities are computed using the mass function from UltraVista (Ilbert et al. 2013). If $M_2 > M_{\text{lim}}$, obviously $w_{\text{comp}} = 1$.

Then, w_θ is computed for each pair as $a/(N_{zz}/N_{\text{pp}})$, where N_{zz} is the number of projected pairs in the spectroscopic catalogue for a given angular separation, N_{pp} is the number of projected pairs in the initial photometric catalogue for the same separation, and a the value of N_{zz}/N_{pp} at large separations. For our survey $w_\theta \sim 1$ for $\theta > 5$ arcsec, and it is lower than 1 at smaller separations when the companion galaxy lies by chance in the slit.

After correcting for the selection function as described above we find $N_p = 216$ and so we derive a measurement for the major merger fraction of $f_{\text{MM}} = 19.4^{+9}_{-6}\%$ for a mean redshift $z = 2.6$ over $1.8 < z < 4.0$. The pair fraction error is estimated by combining the Poisson error on the pair number in quadrature with the errors in w_{comp} estimated using an uncertainty on the mass limit of a factor 1.5.

Because of the number of confirmed spectroscopic pairs and the well controlled selection function, this is one of the best measurements to date at these high redshifts. This value is comparable to values observed from pair identification at lower redshifts $1 < z < 1.8$ in the MASSIV survey (López-Sanjuan et al. 2013), where they found $f_{\text{MM}} = 20.8, 20.1, 22.0\%$ at $z = 1, 1.3, 1.6$, respectively, i.e. similar to our higher redshift value. Measurements have also been obtained from CAS morphological analysis up to $z = 3$ Conselice et al. (2003), who find merger fractions $\sim 10\text{--}40\%$ in the redshift range 2–3 depending on absolute magnitude, with large uncertainties related to photometric redshift estimates and detection of low surface brightness features.

The merger rate can only be derived from the knowledge of the merger time scale of each pair, but this cannot be obtained by direct observation. To derive the merger time scale we use the observed projected spatial and velocity separations, and a 0.2 dex error in mass estimation along with the prescription from Kitzbichler & White (2008) derived from numerical simulations. The merging time scale for each pair is listed in Table 1; with separations from 6 to 25 h^{-1} kpc and mass ratio 1/6 to 1, the average merging time scale of our sample is $\langle T_{\text{merg}} \rangle = 1$ Gyr, and the median is 0.7 Gyr.

These merger time scales are used to infer the merger rate, which is the ratio of the merger fraction to the volume probed by the VUDS and VVDS surveys in the redshift range where pairs are identified. We computed the major merger rate as $R_{\text{MM}} = f_{\text{MM}} \times T_{\text{merg}}^{-1}$, where f_{MM} is as computed above and $T_{\text{merg}} = 1.12$ Gyr from the average T_{merg} in Table 1. After applying the same weighting scheme as for the rest of the analysis, we find a merger rate $R_{\text{MM}} = 0.174^{+0.08}_{-0.05} \text{ Gyr}^{-1}$. We further point out that since our pair sample is not strictly mass-selected, the merger fraction and merger rates derived here are averaged over the mass range considered; investigating variations of the merger fraction with stellar mass will require larger samples than discussed in this paper.

6. Discussion and conclusions: the role of major merging at $2 \lesssim z < 4$

We have identified 12 pairs of galaxies with redshifts $1.81 \leq z \leq 3.65$ from the on-going VUDS combined with the VVDS. Both

components of the pairs have a confirmed spectroscopic redshift obtained with VIMOS on the VLT and, therefore, comprise a unique sample of true physical pairs at these redshifts. The galaxies in our sample span a wide mass range from $10^{9.1} M_\odot$ to $10^{11} M_\odot$. The majority of galaxies in our pairs show signs of strong star formation, a common property at these redshifts, as proved by either strong Ly α emission, strong UV continuum, or both, and with one of them showing AGN activity. The mass ratio of the merger is in the range $1 < M_1/M_2 < 6$, with 11 of 12 pairs satisfying a major merger pair criterion $1 < M_1/M_2 < 4$.

We find a pair fraction $f_{\text{MM}} = 19.4^{+9}_{-6}\%$ and a merger rate $R_{\text{MM}} = 0.174^{+0.08}_{-0.05} \text{ Gyr}^{-1}$. This estimate is the first to use a robust sample of pairs with confirmed spectroscopic redshifts at $2 < z < 4$. Previous work used either morphological indicators (Conselice et al. 2003) or photometric pairs (Bluck et al. 2009), which accumulate several sources of uncertainties different from those associated to spectroscopic pairs, but when taking these into account, our results are in broad quantitative agreement with these studies in identifying a high pair fraction or merger rate at these epochs.

With the merger time scales as derived in Sect. 5, it is interesting to note that most of these pairs will have merged before the peak of star formation at $z \simeq 1.5$ (see e.g. Cucciati et al. 2012). The contribution of these major mergers to the mass growth of individual galaxies is substantial. With an average mass ratio of 1.75 for the 11 major merger pairs, the most massive galaxies involved in these mergers will have increased their stellar mass by $\sim 60\%$ from $z \sim 3$ to $z \sim 1.5$ from the merging process alone.

Our observations therefore provide unambiguous evidence of major merging occurring at $2 \lesssim z < 4$. It is clear that hierarchical assembly, with massive galaxies being built from the merging of less massive ones, is at work at these redshifts and that major merging is contributing to the assembly of mass in galaxies at early times. This mass assembly simply results from the sum of the masses in each galaxy in a merging pair, a simple and effective way to increase mass at each merging event. Minor mergers, with a mass ratio greater than the factor four probed here, are also expected to contribute to this mass growth, but remains unconstrained at these redshifts. An additional increase in stellar mass from star formation triggered by the merging process is also possible, with a range of mass production identified in the literature, ranging from relatively large (e.g. Kocovski et al. 2011) to more limited star bursts (e.g. Mullaney et al. 2012), depending on the duration and strength of the merger induced burst. Merging is therefore a clear path to move low mass galaxies towards the higher end of the mass function, which contributes to the evolution of the stellar mass function (e.g. Ilbert et al. 2013).

These results are to be placed in the context of the currently favoured picture of galaxy assembly, with cold accretion playing a key role in building-up mass in galaxies (e.g. Dekel et al. 2009). As expected in the hierarchical picture of DM halo growth by merging, our results indeed show that galaxies are merging at a high rate and that therefore merging substantially contributes to the build-up of galaxies with high stellar masses before the peak in cosmic star formation activity. A galaxy at $z \sim 1.5$ therefore includes different populations of stars that each may have different ages and chemical enrichment, and may have formed in different environments before integrating their post-merger galaxy. Merging in combination with other mass assembly processes may account for the overall increase with redshift of the stellar mass density of the galaxy

population (Ilbert et al. 2013). The large gas reservoirs identified around high redshift galaxies (Tacconi et al. 2010; Daddi et al. 2010) imply the continuous formation of stars, which could potentially be sustained by new gas brought in from a cold accretion process, although direct observational evidence of accretion remains scarce (Bouché et al. 2013). The total mass growth of a galaxy must therefore come from all these different processes at work in parallel at these epochs. By precisely knowing the contribution of merging to global mass assembly measured e.g. by the growth of the stellar mass density, one would ultimately be able to place upper limits to the total mass growth from other processes, including cold gas accretion.

The integrated contribution of merging processes to the complete history of mass assembly requires knowledge of the evolution of the merger rate since early times (i.e. significantly beyond $z \sim 2$). Building on the sample presented in this paper, the VUDS survey, when complete, will enable a robust measurement of the merging rate out to $z \sim 4$ and an estimate of the total amount of mass assembled by the merging process since the early universe.

Acknowledgements. This work is based in part on data products produced at TERAPIX and the Canadian Astronomy Data Centre as part of the Canada-France-Hawaii Telescope Legacy Survey, a collaborative project of the NRC and CNRS. This work is based on observations taken by the CANDELS Multi-Cycle Treasury Program with the NASA/ESA HST, which is operated by the Association of Universities for Research in Astronomy, Inc., under NASA contract NAS5-26555. We thank the ESO staff for their support and efficient execution of the observation programme. This work is supported by funding from the European Research Council Advanced Grant ERC-2010-AdG-268107-EARLY.

References

- Barnes, J. E., & Hernquist, L. 1992, *ARA&A*, 30, 705
- Bielby, R., Hudelot, P., McCracken, H. J., et al. 2012, *A&A*, 545, A23
- Bluck, A. F. L., Conselice, C. J., Bouwens, R. J., et al. 2009, *MNRAS*, 394, L51
- Bolzonella, M., Kovač, K., Pozzetti, L., et al. 2010, *A&A*, 524, A76
- Bouché, N., Dekel, A., Genzel, R., et al. 2010, *ApJ*, 718, 1001
- Bouché, N., Murphy, M. T., Kacprzak, G. G., et al. 2013, *Science*, 341, 50
- Bournaud, F., Jog, C. J., & Combes, F. 2005, *A&A*, 437, 69
- Bournaud, F., Chapon, D., Teyssier, R., et al. 2011, *ApJ*, 730, 4
- Bruzual, G., & Charlot, S. 2003, *MNRAS*, 344, 1000
- Cattaneo, A., Faber, S. M., Binney, J., et al. 2009, *Nature*, 460, 213
- Conselice, C. J., Bershady, M. A., Dickinson, M., & Papovich, C. 2003, *AJ*, 126, 1183
- Contini, T., Garilli, B., Le Fèvre, O., et al. 2012, *A&A*, 539, A91
- Cooke, J., Berrier, J. C., Barton, E. J., Bullock, J. S., & Wolfe, A. M. 2010, *MNRAS*, 403, 1020
- Cresci, G., Mannucci, F., Maiolino, R., et al. 2010, *Nature*, 467, 811
- Cucciati, O., Tresse, L., Ilbert, O., et al. 2012, *A&A*, 539, A31
- Daddi, E., Bournaud, F., Walter, F., et al. 2010, *ApJ*, 713, 686
- Davis, M., Efstathiou, G., Frenk, C. S., & White, S. D. M. 1985, *ApJ*, 292, 371
- De Lucia, G., Springel, V., White, S. D. M., Croton, D., & Kauffmann, G. 2006, *MNRAS*, 366, 499
- de Ravel, L., Le Fèvre, O., Tresse, L., et al. 2009, *A&A*, 498, 379
- de Ravel, L., Kampczyk, P., Le Fèvre, O., et al. 2011, unpublished [[arXiv:1104.5470](https://arxiv.org/abs/1104.5470)]
- de Vaucouleurs, G., de Vaucouleurs, A., Corwin, H. G., et al. 1991, *Third Reference Catalogue of Bright Galaxies*, Volume 1–3, XII, 2069, 7 figs (New York: Berlin Heidelberg Springer-Verlag)
- Dekel, A., Birnboim, Y., Engel, G., et al. 2009, *Nature*, 457, 451
- Di Matteo, T., Khandai, N., DeGraf, C., et al. 2012, *ApJ*, 745, L29
- Dijkstra, M., & Loeb, A. 2009, *MNRAS*, 400, 1109
- Garilli, B., Fumana, M., Franzetti, P., et al. 2010, *PASP*, 122, 827
- Gawiser, E., van Dokkum, P. G., Herrera, D., et al. 2006, *ApJS*, 162, 1
- Guzzo, L., Scodreggio, M., Garilli, B., et al. 2014, *A&A*, in press, [[DOI 10.1051/0004-6361/201321489](https://arxiv.org/abs/1004.6361)]
- Hopkins, P. F., Hernquist, L., Cox, T. J., et al. 2006, *ApJS*, 163, 1
- Ilbert, O., Arnouts, S., McCracken, H. J., et al. 2006, *A&A*, 457, 841
- Ilbert, O., Salvato, M., Le Floch, E., et al. 2010, *ApJ*, 709, 644
- Ilbert, O., McCracken, H. J., Le Fèvre, O., et al. 2013, *A&A*, 556, A55
- Kacprzak, G. G., Churchill, C. W., Steidel, C. C., Spitler, L. R., & Holtzman, J. A. 2012, *MNRAS*, 427, 3029
- Kauffmann, G., White, S. D. M., & Guiderdoni, B. 1993, *MNRAS*, 264, 201
- Kereš, D., Katz, N., Weinberg, D. H., & Davé, R. 2005, *MNRAS*, 363, 2
- Kereš, D., Katz, N., Fardal, M., Davé, R., & Weinberg, D. H. 2009, *MNRAS*, 395, 160
- Kitzbichler, M. G., & White, S. D. M. 2008, *MNRAS*, 391, 1489
- Kocevski, D. D., Lemaux, B. C., Lubin, L. M., et al. 2011, *ApJ*, 736, 38
- Koekemoer, A. M., Aussel, H., Calzetti, D., et al. 2007, *ApJS*, 172, 196
- Koekemoer, A. M., Faber, S. M., Ferguson, H. C., et al. 2011, *ApJS*, 197, 36
- Le Fèvre, O., Abraham, R., Lilly, S. J., et al. 2000, *MNRAS*, 311, 565
- Le Fèvre, O., Saisse, M., & Mancini, D. 2003, in *SPIE Conf. Ser.* 4841, eds. M. Iye, & A. F. M. Moorwood, 1670
- Le Fèvre, O., Mellier, Y., McCracken, H. J., et al. 2004, *A&A*, 417, 839
- Le Fèvre, O., Vettolani, G., & Garilli, B. 2005, *A&A*, 439, 845
- Le Fèvre, O., Cassata, P., Cucciati, O., et al. 2013a, *A&A*, submitted [[arXiv:1307.6518](https://arxiv.org/abs/1307.6518)]
- Le Fèvre, O., Cassata, P., Cucciati, O., et al. 2013b, *A&A*, 559, A14
- Le Fèvre, O., Tasca, L. A. M., Cassata, P., et al. 2014, *A&A*, submitted [[arXiv:1403.3938](https://arxiv.org/abs/1403.3938)]
- Lemaux, B. C., Le Floch, E., Le Fèvre, O., et al. 2013, *A&A*, submitted [[arXiv:1311.5228](https://arxiv.org/abs/1311.5228)]
- Lilly, S. J., Le Fèvre, O., Renzini, A., & Zamorani, G. 2007, *ApJS*, 172, 70
- Lin, L., Patton, D. R., Koo, D. C., et al. 2008, *ApJ*, 681, 232
- López-Sanjuan, C., Le Fèvre, O., de Ravel, L., et al. 2011, *A&A*, 530, A20
- López-Sanjuan, C., Le Fèvre, O., Tasca, L. A. M., et al. 2013, *A&A*, 553, A78
- Lotz, J. M., Jonsson, P., Cox, T. J., & Primack, J. R. 2010, *MNRAS*, 404, 575
- McCracken, H. J., Milvang-Jensen, B., Dunlop, J., et al. 2012, *A&A*, 544, A156
- Mihos, J. C., & Hernquist, L. 1996, *ApJ*, 464, 641
- Moore, B., Katz, N., Lake, G., Dressler, A., & Oemler, A. 1996, *Nature*, 379, 613
- Mullaney, J. R., Pannella, M., Daddi, E., et al. 2012, *MNRAS*, 419, 95
- Murray, N., Quataert, E., & Thompson, T. A. 2005, *ApJ*, 618, 569
- Patton, D. R., Carlberg, R. G., Marzke, R. O., et al. 2000, *ApJ*, 536, 153
- Popesso, P., Dickinson, M., Nonino, M., et al. 2009, *A&A*, 494, 443
- Scodreggio, M., Franzetti, P., Garilli, B., et al. 2005, *PASP*, 117, 1284
- Scoville, N., Aussel, H., Brusa, M., et al. 2007, *ApJS*, 172, 1
- Silk, J. 1997, *ApJ*, 481, 703
- Silk, J., & Mamon, G. A. 2012, *Res. Astron. Astrophys.*, 12, 917
- Springel, V., Di Matteo, T., & Hernquist, L. 2005a, *MNRAS*, 361, 776
- Springel, V., White, S. D. M., Jenkins, A., et al. 2005b, *Nature*, 435, 629
- Steidel, C. C., Erb, D. K., Shapley, A. E., et al. 2010, *ApJ*, 717, 289
- Sulentic, J. W., & Tift, W. G. 1973, *The revised new general catalogue of non-stellar astronomical objects* (Tucson: University of Arizona Press)
- Tacconi, L. J., Genzel, R., Neri, R., et al. 2010, *Nature*, 463, 781
- Taniguchi, Y., Scoville, N., Murayama, T., et al. 2007, *ApJS*, 172, 9